Taylor & Francis
Taylor & Francis Group

CLINICAL STUDY

OPEN ACCESS | Check for updates

Prediction of peripheral blood lymphocyte subpopulations after renal transplantation

Bo Peng[a,b*], Xuyu Xiang[a,b*], Han Tian[c], Kaiqiang Xu[d], Quan Zhuang[a,b], Junhui Li[a,b], Pengpeng Zhang[a,b], Yi Zhu[a,b], Min Yang[a,b], Jia Liu[a,b], Yujun Zhao[a,b], Ke Cheng[a,b] and Yingzi Ming[a,b] (iD)

[a]Transplantation Center, The Third Xiangya Hospital, Central South University, Changsha, China; [b]Engineering and Technology Research Center for Transplantation Medicine of National Health Commission, Central South University, Changsha, China; [c]School of Computer Science and Technology, University of Science and Technology of China (USTC), Hefei, China; [d]iSING Lab, Hong Kong University of Science and Technology, Hong Kong, China

ABSTRACT

Immune monitoring is essential for maintaining immune homeostasis after renal transplantation (RT). Peripheral blood lymphocyte subpopulations (PBLSs) are widely used biomarkers for immune monitoring, yet there is no established standard reference for PBLSs during immune reconstitution post-RT. PBLS data from stable recipients at various time points post-RT were collected. Binary and multiple linear regressions, along with a mixed-effect linear model, were used to analyze the correlations between PBLSs and clinical parameters. Predictive models for PBLS reference values were developed using Gradient Boosting Regressor, and the models' performance was also evaluated in infected recipients. A total of 1,736 tests from 494 stable recipients and 98 tests from 82 infected recipients were included. Age, transplant time, induction therapy, dialysis duration, serum creatinine, albumin, hemoglobin, and immunosuppressant drug concentration were identified as major factors influencing PBLSs. CD4$^+$ and CD8$^+$ T cells and NK cells increased rapidly, stabilizing within three months post-RT. In contrast, B cells peaked at around two weeks and gradually plateaued after four months. Both static and dynamic predictive models provided accurate reference values for PBLSs at any time post-RT, with the static model showing superior performance in distinguishing stable, infected and sepsis patients. Key factors influencing PBLS reconstitution after RT were identified. The predictive models accurately reflected PBLS reconstitution patterns and provided practical, personalized reference values for PBLSs, contributing to precision-guided care. The study was registered on Chinese Clinical Trial Registry (ChiCTR2300068666).

1. Introduction

Renal transplantation (RT) is an effective treatment for end-stage renal disease (ESRD), but postoperative immunosuppression is routinely required for renal transplant recipients (RTRs). Currently, immunosuppressive drugs, primarily calcineurin inhibitors (CNIs), are dosed based on weight and adjusted according to drug concentration. However, drug concentration alone does not directly reflect the host's immune status, and clinical outcomes can vary significantly among individuals, even with similar drug levels. In contrast, immune monitoring using appropriate biomarkers can directly assess immune function, enabling a shift from empirical immunosuppressive treatment to precision-guided care tailored to each patient.

Several biomarkers have been identified for immune monitoring in RTRs [1–3]. Due to considerations of technical difficulty, laboratory hands-on time, and cost, peripheral blood lymphocyte subpopulations (PBLSs)—including CD4$^+$ T cells, CD8$^+$ T cells [4], B cells, and natural killer (NK) cells [5]—have become the most widely used biomarkers in transplantation centers. Previous studies have demonstrated that PBLS monitoring can aid in clinical diagnosis, treatment decisions, and prognosis prediction for infection in RTRs [6–9].

Unlike in healthy individuals, where PBLS reference values are relatively stable [10], the situation in RTRs is more complicated. Induction therapy, particularly T cell-depleting agents like anti-thymocyte globulin (ATG), significantly impacts the numbers of both T and non-T cells [11]. Consequently, PBLS levels often drop to nearly zero during

Supplemental data for this article can be accessed online at https://doi.org/10.1080/0886022X.2025.2493231.

the perioperative period and gradually recover post-transplantation, a process known as immune reconstitution in RTRs [12]. Additionally, ongoing immunosuppressive regimens further suppress immune cell proliferation, rendering the reference values for healthy individuals inapplicable to RTRs. The absence of accurate reference values for RTRs limits the clinical utility of PBLSs in immune monitoring.

To address this gap, we collected a large dataset of PBLS measurements during immune reconstitution in RTRs and used machine learning techniques to develop predictive models. The patterns and influencing factors of immune reconstitution in stable RTRs were identified, and the predictive models demonstrated effectiveness in identifying RTRs with infections based on predicted PBLS values.

2. Materials and methods

2.1. Study design and population

This retrospective study enrolled patients who underwent PBLS tests from January 1st, 2017 to December 31st, 2021 in our center. The inclusion criteria were as follows: (1) patients received RT from deceased organ donation (DD) [13] in our center after January 1st, 2015, or from close family members; (2) patients had complete clinical information during the perioperative period and follow–up; (3) age ranged from 18 to 70 years; (4) no multiple–organ transplantation. The stable RTRs were defined as follows: (1) no infection when receiving the test; (2) no delayed graft function (DGF) or rejection during the perioperative period; (3) patients had stable allograft function (serum creatine ≤ 176 μmol/L) without clinical manifestations of rejection during the non–perioperative period.

RTRs diagnosed with infection were also included to validate the predictive model for differentiating stable and infected patients. Diagnostic criteria of infection (pneumonia, urinary infection or other infections) were as follows: (1) obvious clinical symptoms including fever, cough, pollakiuria, diarrhea, etc.; (2) positive laboratory tests including blood routine examination, serum procalcitonin, (1–3)–beta–D–glucan/galactomannan test (G/GM test) or pathogenic evidence; (3) significant imaging findings from X–ray or computed tomography (CT) [14]. Sepsis was defined according to the Sepsis-3 criteria, and organ dysfunction was assessed using a Sequential Organ Failure Assessment (SOFA) score of 2 points or more. Given that stable RTRs may maintain relatively poorer renal function compared to healthy control, strict use of the SOFA score to assess renal function could lead to an overestimation of infection severity. Therefore, only KTRs with a creatinine level of 171 mmol/L or higher (SOFA score ≥ 2 points for renal function), or those with a noticeable increase in creatinine during infection, were classified as having renal dysfunction for SOFA scoring purposes [14]. All infected RTRs received the PBLS test within 24 h after admission.

All the DD transplants performed in our center were approved by the DD Ethics Committee of the Third Xiangya Hospital, Central South University. None of the organs were procured from executed prisoners and that organs were procured after informed consent or authorization. All DD in this study were China category I cases, which aligned with the internationally standardized criteria for brain death organ donation [15,16]. The study was approved by the Institutional Review Board of Third Xiangya Hospital, Central South University (22294), and registered on Chinese Clinical Trial Registry (ChiCTR2300068666).

2.2. Immunosuppression

ATG (rabbit ATG, a total of 2 – 3 mg/kg) or basiliximab (20 mg at days 0 and 4) was used for induction therapy. In general, ATG was administrated for patients with high risk of delayed graft function (DGF) or rejection, such as existence of donor-specific antibodies (DSA) or high level of panel reactive antibodies (PRA), and receiving allografts from DD or extended criteria donors. Basilixmab was administrated for the low-risk patients (no preexistence of HLA antibody, receiving allograft from living relatives). The standard triple immunosuppressive regimens including CNI (tacrolimus or cyclosporine A (CsA)), mycophenolate mofetil (MMF, 0.75 g per 12 h during perioperative period and 0.5 g per 12 h for maintenance) or entericcoated mycophenolate sodium (EC-MPS, 0.54 g per 12 h during perioperative period and 0.36 g per 12 h for maintenance), and corticosteroids (methylprednisolone 500 mg during operation, 250 – 300 mg on day 1 and day 2, and 120 – 160 mg on day 3; prednisone 20 mg since day 4 and gradually reduced to 5 mg) were given as the anti-rejection regimens. The target trough level of tacrolimus was 8 – 10 ng/ml for the first month and 5 – 8 ng/ml for maintenance. The target trough level of CsA was 200 – 300 ng/ml for the first month and 100 – 200 ng/ml for maintenance.

2.3. Immune monitoring panel for PBLSs

The BD Multitest 6–color TBNK reagent with BD Trucount tube which identified the percentages and absolute counts of total lymphocytes (namely TBNK), $CD3^+$ T cells, $CD3^+CD4^+$ T cells, $CD3^+CD8^+$ T cells, $CD19^+$ B cells and $CD16^+/CD56^+$ NK cells was used for PBLS test. This panel was performed according to the manufacturer's instructions and analyzed by BD FACSCanto clinical software (BD BioSciences, San Jose, CA, USA).

During the perioperative period, RTRs routinely received the PBLS test every week in our center, or based on clinical need. During follow–up, stable RTRs were advised to receive 1 – 3 PBLS tests within the first–year post transplantation.

2.4. Machine learning model building

In order to develop predictive models for the reference values of PBLSs, relevant clinical parameters were classified into the static and dynamic indicators. Static indicators remained constant over time, which included age, gender, type of dialysis, dialysis duration, donor source (DD or living relatives), induction therapy, and the maintenance regimen. Static

indicators provided a baseline understanding of a patient's typical recovery trajectory post–transplantation. Dynamic indicators were derived from clinical results obtained at each examination and reflected the real–time status of the patient, which included transplant time, serum creatinine (Scr), blood urea nitrogen (BUN), blood uric acid, trough CNI drug concentration, albumin, hemoglobin (Hb), and estimated glomerular filtration rate (eGFR).

The static predictive model used only static indicators. We stratified the dataset by segmenting it based on specific target values of a key indicator and then proceeded to calculate the average model output for each stratified subgroup, ensuring a focused evaluation of model performance across different levels of the indicator. In contrast, the dynamic model incorporated dynamic results to provide a more immediate assessment. Specifically, the dynamic model adopted a window of historical dynamic indicators from the last ($k=3$) clinic examinations as the model input. This technique was essential in time series analysis and machine learning, allowing the model to capture temporal dynamics inherent in sequential data. Both models employed Gradient Boosting Regressor, a machine learning algorithm for regression tasks. It sequentially built a series of decision trees, each correcting the errors of its predecessors. This method, rooted in optimizing a loss function through gradient descent, excelled in capturing complex patterns in data.

In the static model, we also identified the inflection points using a specialized algorithm. The algorithm discerned the overall data trend (increasing or decreasing) and located a significant shift in this trend based on specific numerical thresholds. For an increasing trend, the algorithm found an inflection point where the rate of change shifted from being steep to less steep. This was quantitatively defined as a point where the average rate of change over two points decreased from being above a threshold (e.g., a 30–degree slope equivalent) to below this threshold. Conversely, in a decreasing trend, the change point was identified where the rate of change shifted from less steep to steeper, using similar slope criteria but in the opposite direction.

The predictive models were available for free on the website http://pbls.kqxu.com/. When inputted the required clinical parameters from a certain patient, the predicted PBLS reference values for this patient would be calculated and presented.

2.5. Predictive model evaluation

For our training procedure, 80% of the data was randomly selected for training and the remaining 20% was for validation. A grid search optimized each model's configuration, including the number of trees, tree depth limit, and leaf split criterion. Evaluation metrics included mean error, mean absolute error, and the mean ratio of absolute error, alongside the proportion of the results falling within a 90% confidence interval and the mean percentile in the confidence interval.

$$\text{Mean error} = \sum(true\ value - predicted\ value) / n$$

$$\text{Mean absolute error} = \sum |true\ value - predicted\ value| / n$$

$$\text{Mean ratio of absolute error} = Mean\ absolute\ error\ /\ mean\ true\ value$$

2.6. Statistical analysis

The Wilcoxon rank–sum test, unpaired t–test, paired t–test, and chi–square test were used appropriately to evaluate the significance of differences in data between groups. Binary linear regression, multiple linear regression, and mixed effect linear models were used to analyze the correlation between PBLSs and clinical information. A p–value < 0.05 was considered statistically significant. All statistical analyses were performed using R (4.3.1, Posit Software, Boston, MA, USA), SPSS software 26 (IBM, Chicago, IL, USA), or Graphpad Prism 8 (Graphpad Software, San Diego, CA, USA).

3. Results

3.1. Patient characteristics

A total of 8,014 PBLS tests were recorded. After applying the inclusion criteria, 494 stable RTRs, accounting for 1,736 tests, were enrolled. Additionally, 82 infected RTRs with 98 tests were included. The study flowchart is depicted in Figure 1.

The demographic characteristics of the patients were detailed in Table 1. Approximately 80% of patients received ATG as induction therapy. Moreover, the majority of patients received allografts from DD ($n=454$, 91.90%) and were maintained on tacrolimus ($n=480$, 97.17%). Clinical data related to these PBLS tests were presented in Table 2. The dataset showed a sufficient sample size distribution across various post-transplant periods. Given that PBLSs in RTRs changed markedly during the perioperative period and that immune reconstitution primarily occurred in the early post-transplantation stage, data within 90 days post-transplant accounted for more than half of the dataset ($n=996$, 57.37%). Data beyond 365 days were classified into one group.

Statistical data on PBLSs over different post-transplant periods were illustrated in Figure 2 and Supplementary Table 1. The results demonstrated considerable variability, even when stratified by transplant time and induction therapy. The wide intervals observed in the results rendered them unsuitable as reference values for clinical practice, underscoring the need for a more precise predictive model of PBLSs.

3.2. The influence factors of immune reconstitution after RT

To identify factors influencing immune reconstitution post-RT, multiple linear regression, binary linear regression, and mixed-effect linear models were employed to analyze the correlation between clinical parameters and PBLSs. Multiple linear regression analysis provided an overview of each factor's impact on PBLSs (Supplementary Table 2). The analysis revealed that clinical parameters including age, induction therapy, dialysis duration, Scr, BUN, albumin, and Hb were
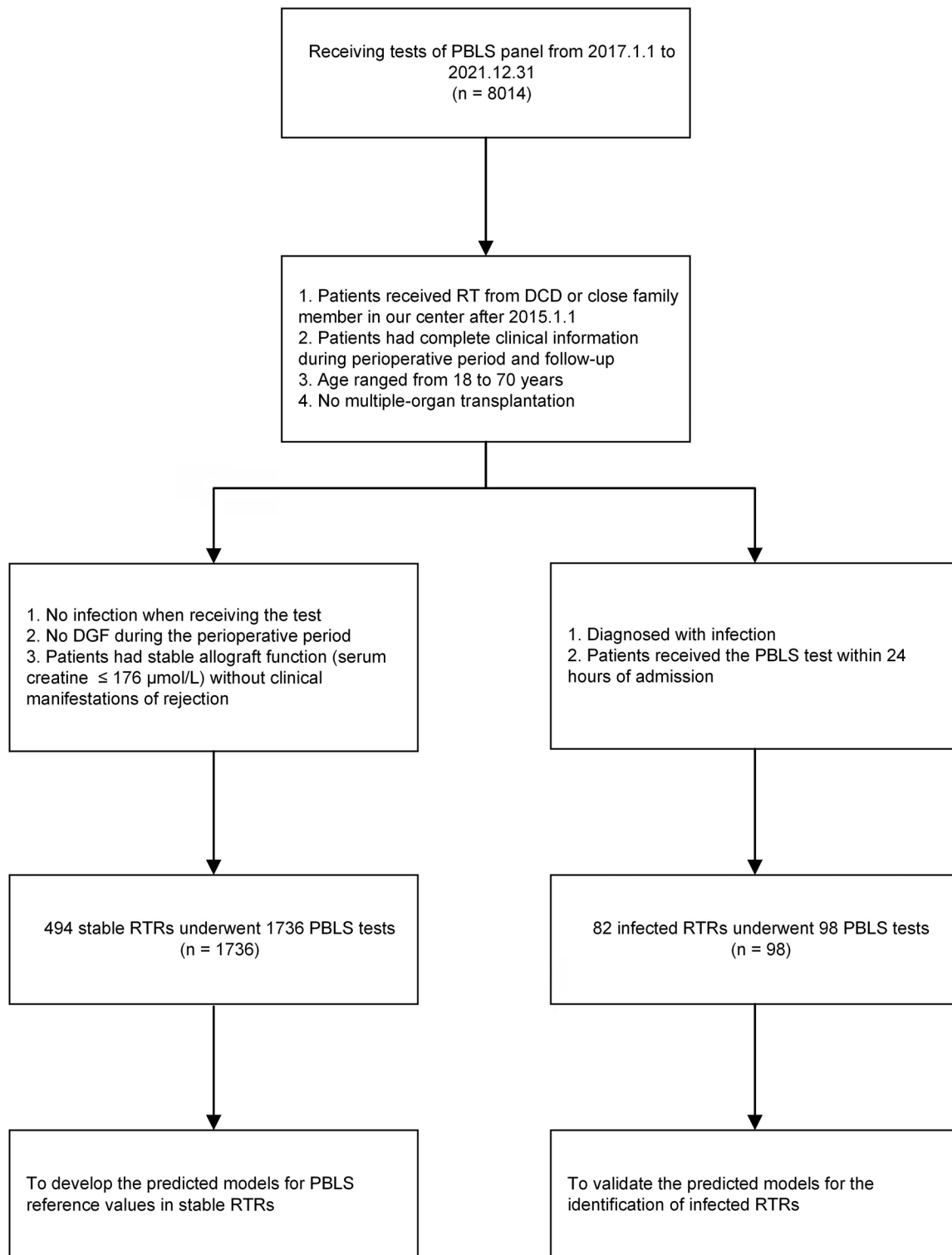
Figure 1. The flowchart of the study. PBLS, peripheral blood lymphocyte subpopulation. RT, renal transplantation. DD, donation after citizen's death. DGF, delayed graft function. RTRs, renal transplantation recipients.

significantly correlated with TBNK and at least four other PBLS parameters. The use of ATG as induction therapy was strongly and negatively correlated with all PBLS parameters. Notably, transplant time did not significantly correlate with TBNK or CD4$^+$ T cells.

Further binary linear regression analysis, stratified by induction therapy, was conducted to assess the correlation between

transplant time and PBLSs (Supplementary Table 3). Transplant time was significantly correlated with TBNK and four other parameters at 0 – 7 days and 14 – 30 days postoperatively. In the ATG subgroup, CD3$^+$ T cells and CD8$^+$ T cells were notably associated with transplant time one year post-RT.

Similarly, the correlation between induction therapy and PBLSs across different time periods was analyzed (Supplementary

Table 1. Patient characteristics.

	Stable patient ($n=494$)	Infected patient ($n=82$)	p value
Common characteristics			
Age (years)	41.00 (33.00–49.00)	41.00 (32.00–50.00)	0.8313
Male, n (%)	309 (62.55%)	40 (48.78%)	0.0181
Number of included tests, n (%)			<0.0001
1–2	263 (53.24%)	82 (100.00%)	
3–5	133 (26.92%)	0 (0.00%)	
6–10	76 (15.38%)	0 (0.00%)	
>10	22 (4.45%)	0 (0.00%)	
Pre-transplant data			
Etiology of underlying ESRD, n (%)			0.5370
Glomerulonephritis	30 (6.07%)	3 (3.66%)	
Diabetic nephropathy	3 (0.61%)	0 (0.00%)	
Other	28 (5.67%)	7 (8.54%)	
Unknown	436 (88.26%)	72 (87.80%)	
Type of dialysis, n (%)			0.3434
Hemodialysis	340 (68.83%)	62 (75.61%)	
Peritoneal dialysis	127 (25.71%)	18 (21.95%)	
Without dialysis	27 (5.47%)	2 (2.44%)	
Dialysis duration (days)	492.00 (265.00–962.00)	458.00 (168.00–1429.00)	0.8537
Post-transplant data			
Donor, n (%)			0.2222
DD	454 (91.90%)	72 (87.80%)	
Relative	40 (8.10%)	10 (12.20%)	
Induction therapy, n (%)			0.2692
ATG	394 (79.76%)	61 (74.39%)	
Non–ATG	100 (20.24%)	21 (25.61%)	
CNI, n (%)			0.3245
Tacrolimus	480 (97.17%)	78 (95.12%)	
CsA	14 (2.83%)	4 (4.88%)	
Retransplantation, n (%)	19 (3.85%)	2 (2.44%)	0.5290

Normally distributed data was presented as mean ± SD, non–normally distributed data was presented as median (25th percentile – 75th percentile).

DD, donation after citizens' death; RT, renal transplantation; ATG, anti–thymocyte globulin; CNI, calcineurin inhibitor; Scr, serum creatinine; eGFR, estimated glomerular filtration rate; BUN, blood urea nitrogen; Hb, hemoglobin; SD, standard deviation.

Table 2. Test characteristics.

	Stable test ($n=1736$)	Infected test ($n=98$)	p value
Transplant time (days)	60.00 (17.00–284.00)	313.00 (123.00–758.00)	<0.0001
0–7 days, n (%)	151 (8.70%)	0 (0%)	
7–14 days, n (%)	222 (12.79%)	0 (0%)	
14–30 days, n (%)	250 (14.40%)	2 (2.04%)	
30–90 days, n (%)	373 (21.49%)	16 (16.33%)	
90–180 days, n (%)	186 (10.71%)	19 (19.39%)	
180–365 days, n (%)	198 (11.41%)	15 (15.31%)	
>365 days, n (%)	356 (20.51%)	46 (46.94%)	
Scr (μmol/ L)	110.00 (86.00–136.00)	110.00 (94.00–139.00)	0.1829
eGFR (ml/ min/ 1.73 m^2)	68.02 (50.59–89.69)	68.12 ± 25.59	0.3162
BUN (mmol/ L)	9.05 (6.50–13.43)	8.34 (5.63–12.41)	0.0488
Blood uric acid (μmol/ L)	347.00 (281.00–415.00)	362.50 ± 100.10	0.0941
Albumin (g/ L)	43.90 (39.45–47.70)	39.32 ± 5.82	<0.0001
Hb (g/ L)	112.00 (95.00–130.00)	117.60 ± 28.54	0.2412
CNI drug concentration (C_0)			
Tacrolimus (ng/mL)	7.00 (5.60–8.60)	5.90 (4.55–7.80)	0.0002
CsA (ng/mL)	147.00 (103.50–201.50)	/	

Normally distributed data was presented as mean ± SD, non–normally distributed data was presented as median (25th percentile – 75th percentile).

DD, donation after citizens' death; RT, renal transplantation; ATG, anti–thymocyte globulin; CNI, calcineurin inhibitor; Scr, serum creatinine; eGFR, estimated glomerular filtration rate; BUN, blood urea nitrogen; Hb, hemoglobin; SD, standard deviation; C_0, trough concentration.

Table 4). The results indicated that the correlation between induction therapy and PBLSs evolved over time. ATG significantly reduced PBLSs, except for B cells, within the first three months post-RT. Additionally, ATG had a prolonged effect on CD4+ T cells throughout the study period, with the most significant impact observed in the first three months. Violin plots illustrating PBLSs stratified by induction therapy are shown in Figure 2.

Since some patients underwent multiple tests, a mixed-effect linear model was applied for further analysis. Interaction effects between transplant time and induction therapy, as well as between CNI and drug concentration, were considered (Table 3). Age, induction therapy, dialysis duration, Scr, albumin, and Hb remained significantly correlated with TBNK and at least four other PBLSs. Furthermore, CNI drug concentration, but not the type of CNI, was
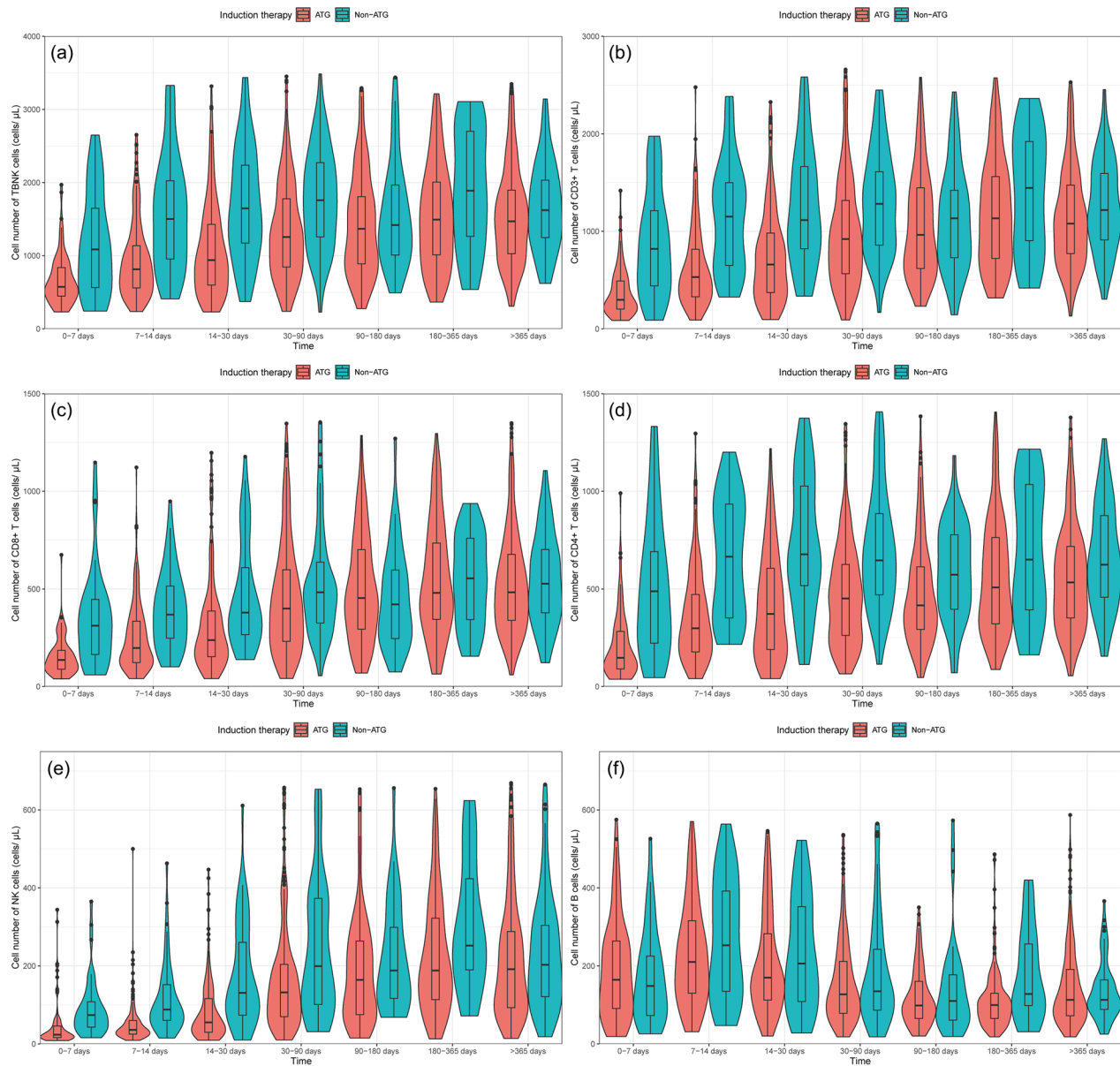
Figure 2. The violin plots of PBLSs at different periods after RT. The data was from stable RTRs and stratified by induction therapy (ATG or non–ATG). (a). The cell number of TBNK. (b). The cell number of CD3+ T cells. (c). The cell number of CD4+ T cells. (d). The cell number of CD8+ T cells. (e). The cell number of NK cells. (f). The cell number of B cells. PBLSs, peripheral blood lymphocyte subpopulations. TBNK, a total of CD3+ T cells, B cells, and NK cells. RT, renal transplantation. ATG, anti–thymocyte globulin. NK, natural killer.

significantly correlated with TBNK. Interaction effects between transplant time and induction therapy, and between CNI and drug concentration, also significantly influenced TBNK, CD4+ T cells, and B cells. However, changes in CD8+ T cells during immune reconstitution were primarily driven by induction therapy. Significant factors were selected for the further development of predictive models.

3.3. The patterns and inflection points of immune reconstitution identified by the static predictive model

The static predictive model was developed using relevant static indicators, including age, gender, donor source, induction therapy, maintenance regimen, type of dialysis, and dialysis duration. The number of each PBLS was predicted over transplant time. When focusing on a key indicator, other indicators were averaged as described in the methods section. As shown in Figure 3, induction therapy had a strong effect on each PBLS. The ATG subgroup exhibited significantly lower PBLS numbers, particularly in the early post-RT stage. This difference was most pronounced and prolonged in CD4+ T cells. Similar results were observed in the analysis of donor source (Supplementary Figure 1), as the majority of DD transplants received ATG ($n=1343$, 83.2%), while most relative transplants did not ($n=77$, 63.1%). Patients who did not receive dialysis before RT had higher T cell (mainly CD8+ T cells) and B cell counts than those who underwent dialysis, with minimal difference observed between hemodialysis and peritoneal dialysis (Supplementary Figure 2). The longer the dialysis duration,

Table 3. Linear mixed model analysis between general and clinical information and PBLSs.

	TBNK (cells/ µL)		CD3+T (cells/ µL)		CD8+T (cells/ µL)		CD4+T (cells/ µL)		NK (cells/ µL)		B (cells/ µL)	
	β	p value	β	p value	β	p value	β	p value	β	p value	β	p value
Age	−9.83	<0.001	−8.54	<0.001	−5.79	<0.001	−2.19	0.06	1.62	<0.001	−2.54	<0.001
Male vs Female	−1.65	0.98	−37.78	0.43	−41.35	0.11	−0.004	1.00	20.53	0.02	24.23	0.03
DD vs Relative	95.49	0.39	44.88	0.60	62.31	0.19	−19.00	0.68	−8.00	0.66	5.67	0.77
Transplant time	0.27	<0.001	0.18	<0.001	0.05	0.06	0.12	<0.001	0.11	<0.001	−0.0004	0.98
Non–ATG vs ATG	484.94	<0.001	371.17	<0.001	83.45	0.01	289.05	<0.001	78.62	<0.001	49.93	<0.01
Induction therapy * Transplant time	−0.41	<0.01	−0.28	<0.01	−0.08	0.11	−0.20	<0.001	−0.10	0.10	−0.09	<0.01
CsA vs FK506	−143.53	0.43	−21.83	0.88	33.10	0.67	−51.84	0.46	−90.82	0.03	−58.72	0.06
Concentration	12.14	0.02	8.02	0.06	1.69	0.47	6.94	0.00	−1.32	0.31	3.89	<0.001
CNI * Concentration	−11.26	0.04	−7.46	0.08	−1.73	0.47	−6.40	0.00	1.48	0.27	−3.72	<0.001
Etiology												
Unknown vs Other	154.20	0.53	165.34	0.39	142.44	0.18	17.95	0.86	37.47	0.42	−36.02	0.42
Glomerulonephritis vs Other	186.90	0.48	165.18	0.43	143.63	0.21	−7.57	0.95	50.01	0.31	−6.44	0.90
Diabetic nephropathy vs Other	−374.64	0.37	−390.99	0.24	−124.11	0.49	−245.71	0.17	154.53	0.01	−87.53	0.32
Type of dialysis												
Hemodialysis vs Without dialysis	−107.95	0.35	−117.05	0.20	−61.71	0.22	−12.60	0.80	13.04	0.41	25.80	0.23
Peritoneal dialysis vs Without dialysis	−1.95	0.99	−55.68	0.57	−38.05	0.48	19.35	0.72	27.17	0.11	28.64	0.21
Dialysis duration	−0.12	<0.01	−0.07	0.04	−0.03	0.10	−0.04	0.03	−0.02	0.01	−0.03	<0.001
Retransplantation	−168.97	0.55	−293.83	0.18	−211.33	0.08	−27.25	0.82	−14.21	0.78	98.40	0.06
Scr	−0.71	<0.001	−0.56	<0.001	−0.22	<0.01	−0.31	<0.001	−0.07	0.07	−0.10	<0.01
BUN	−2.52	0.25	−4.04	0.02	−2.27	0.02	−1.78	0.04	−1.13	0.03	2.54	<0.001
Blood uric acid	0.53	<0.01	0.49	<0.001	0.30	<0.001	0.17	0.02	0.17	<0.001	−0.07	0.04
Albumin	32.46	<0.001	22.43	<0.001	11.18	<0.001	9.55	<0.001	9.54	<0.001	−0.77	0.24
Hb	4.92	<0.001	4.20	<0.001	2.69	<0.001	1.19	0.00	1.23	<0.001	−0.81	<0.001
eGFR	2.47	<0.001	2.02	<0.001	0.82	0.01	1.04	<0.001	0.04	0.79	0.19	0.13

TBNK is a total of CD3+ T cells, NK cells and B cells.PBLSs, peripheral blood lymphocyte subpopulations; DD, donation after citizen's death; ATG, antihuman thymocyte globulin; CNI, calcineurin inhibitor; Scr, serum creatinine; eGFR, estimated glomerular filtration rate; BUN, blood urea nitrogen; Hb, hemoglobin.

the lower the PBLS counts (Supplementary Figure 3). Interestingly, patients on tacrolimus as the maintenance regimen had higher PBLS counts compared to those on CsA (Supplementary Figure 4). Age also influenced immune reconstitution, primarily for T cells, with younger patients (< 50 years) having higher T cell counts than those aged > 50 years (Supplementary Figure 5). Gender did not significantly affect PBLS immune reconstitution (data not shown).

Despite the impact of several static indicators on immune reconstitution, the trends in the curves remained consistent. T cells and NK cells rapidly increased post-RT and gradually plateaued. The inflection point for CD4+ T cell reconstitution was at 29 days post-RT in the ATG subgroup and 25 days in the non-ATG subgroup. In contrast, CD8+ T cell reconstitution occurred later, with an inflection point at 85 days post-RT in both the ATG and non-ATG groups. The inflection points for NK cell reconstitution occurred around 50 days post-RT. The reconstitution pattern for B cells differed significantly. B cells rapidly increased to a peak around 15 days post-RT, then decreased, eventually plateauing at approximately 125 days. Notably, the plateau level was lower than the initial B cell count.

The performance of the static predictive model was evaluated using the validation dataset (20% randomly selected cases). As shown in Table 4, approximately 80% of the data for each PBLS fell within the 90% predicted intervals, indicating good accuracy. The highest accuracy was observed for

NK cells (85.1%), while the lowest was for CD4+ T cells (78.4%). Precision, assessed by the mean absolute error and the mean ratio of absolute error, indicated that NK cells had the highest deviation, while TBNK had the lowest (mean ratio of absolute error 0.67 and 0.38, respectively).

3.4. More precise reference values of PBLSs predicted by the dynamic predictive model

To further improve the performance, dynamic indicators, detected concurrently with PBLSs, were included in the dynamic predictive model. According to mixed-effect linear model analysis, dynamic indicators including CNI drug concentration, Scr, BUN, blood uric acid, albumin, Hb, and eGFR were utilized for model building. As shown in Table 5, over 80% of the validation dataset data fell within the 90% predicted intervals. The mean absolute error and the mean ratio of absolute error were significantly reduced for each PBLS in the dynamic predictive model compared to the static model (p = 0.01 and p < 0.01, respectively, as tested by paired t-test), providing more precise reference values for clinical practice.

3.5. The performance of the static and dynamic predictive models on infected RTRs

Both the static and dynamic predictive models were developed using data from stable RTRs. A separate cohort of
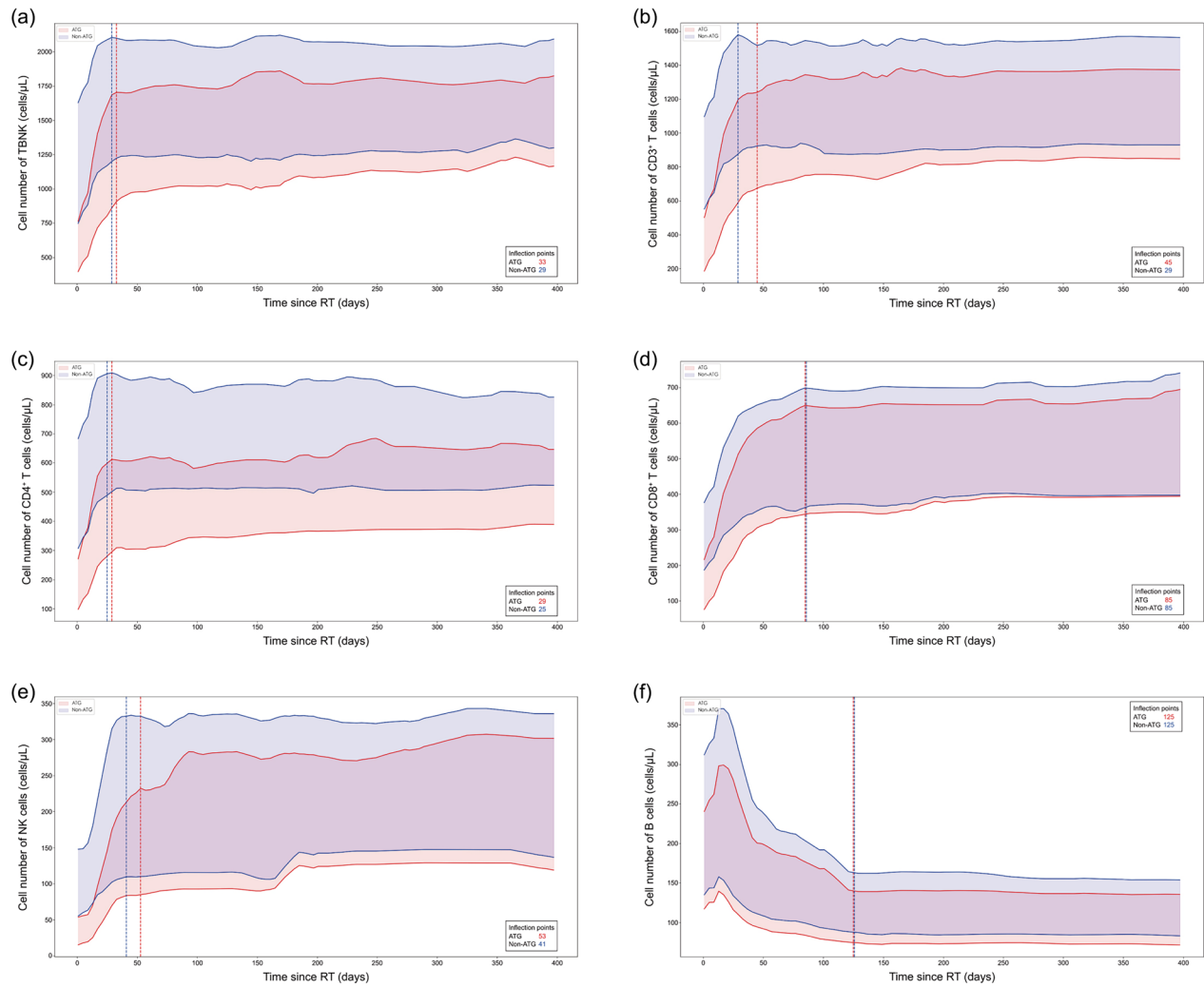
Figure 3. The predicted 90% confidence interval of PBLSs over transplant time and the inflection points identified by the static predictive model. The results were stratified by the induction therapy (ATG or non–ATG) and the average model output was calculated with other static indicators. (a). The predicted cell number of TBNK. (b). The predicted cell number of CD3+ T cells. (c). The predicted cell number of CD4+ T cells. (d). The predicted cell number of CD8+ T cells. (e). The predicted cell number of NK cells. (f). The predicted cell number of B cells. The intersection of the dashed and solid lines marks the inflection points of the curves, where the slope stabilizes markedly. The definition of inflection points is detailed in the methods section, with their time point indicated in the lower right corner of the figure. In all graphs, the red features represent the group that received ATG. PBLSs, peripheral blood lymphocyte subpopulations. TBNK, a total of CD3+ T cells, B cells, and NK cells. RT, renal transplantation. ATG, anti–thymocyte globulin. NK, natural killer.

infected RTRs, characterized by significantly lower PBLS counts compared to stable RTRs (Supplementary Table 5), was recruited for validation. The model performance is presented in Tables 4 and 5.

In the static predictive model, the results for infected RTRs displayed marked skewing. Approximately 70% of the predictions fell within the 90% predicted interval, significantly lower than the proportion for stable RTRs ($p < 0.01$). The mean percentile of the infected cohort was around the 30th percentile ($p < 0.001$), and the mean error was significantly reduced ($p = 0.02$), reflecting the lower PBLS counts in this group. Despite the lower PBLS counts, the mean absolute error did not show a significant difference ($p = 0.22$); however, the mean ratio of absolute error was significantly higher for infected RTRs compared to stable RTRs ($p < 0.01$).

Given the strong discriminatory power of the static model to identify infection, it was further applied to distinguish between sepsis and non-sepsis cases (Table 6). Among 98 infection cases, 14 were diagnosed with sepsis. There was no significant difference in the infection sites between the two groups. The mean percentile was used to assess the model's ability to differentiate between the groups. The sepsis subgroup had significant lower percentiles across all parameters. Therefore, infection patients with lower percentiles in the static predictive model indicated severer infection.

The dynamic predictive model incorporated dynamic indicators, some of which exhibited infection-specific characteristics (Table 2). After adjusting for these dynamic indicators, the model demonstrated comparable performance in predicting PBLSs for infected RTRs, with an accuracy of approximately 80%, not significantly different from that of stable RTRs ($p = 0.14$). Although the mean percentile of the infected group was lower ($p = 0.02$), the mean ratio of absolute error

Table 4. The evaluation of the static predictive model.

Groups	Evaluation indicators	Cell populations					
		TBNK	CD3+ T cells	CD4+ T cells	CD8+ T cells	NK cells	B cells
Stable group	Results within 90% predicted interval (%)	83.1	83.1	78.4	84.5	85.1	82.4
	Mean percentile in predicted interval (%)	49.5	47.3	48.6	46.1	49.4	54.0
	Mean error (cells/μL)	−89.1	−117.5	−33.6	−41.8	4.0	14.2
	Mean absolute error (cells/μL)	518.2	395.5	245.2	184.3	121.3	100.6
	Mean ratio of absolute error	0.38	0.42	0.48	0.46	0.67	0.50
Infected group	Results within 90% predicted interval (%)	68.3	67.1	67.1	75.6	79.3	70.7
	Mean percentile in predicted interval (%)	29.9	30.9	31.3	31.5	38.7	33.5
	Mean error (cells/μL)	−458.7	−338.7	−160.6	−165.7	−66.9	−38.7
	Mean absolute error (cells/μL)	602.5	462.3	236.3	241.4	119.3	68.4
	Mean ratio of absolute error	0.57	0.58	0.61	0.68	0.76	0.77

TBNK is a total of CD3+ T cells, NK cells and B cells.

Table 5. The evaluation of the dynamic predictive model.

Groups	Evaluation indicators	Cell populations					
		TBNK	CD3+ T cells	CD4+ T cells	CD8+ T cells	NK cells	B cells
Stable group	Results within 90% predicted interval (%)	81.7	82.0	84.3	83.7	82.0	82.0
	Mean percentile in predicted interval (%)	51.1	50.9	49.7	52.0	51.4	49.3
	Mean error (cells/μL)	90.9	67.5	21.5	53.2	31.6	21.3
	Mean absolute error (cells/μL)	424.0	318.5	172.1	161.8	86.6	69.4
	Mean ratio of absolute error	0.31	0.33	0.35	0.36	0.47	0.42
Infected group	Results within 90% predicted interval (%)	79.6	81.6	74.5	83.7	81.6	78.6
	Mean percentile in predicted interval (%)	42.9	43.7	43.4	49.3	51.7	35.4
	Mean error (cells/μL)	−216.4	−160.3	−98.3	−58.4	13.9	−26.0
	Mean absolute error (cells/μL)	389.0	312.8	171.1	150.2	77.4	54.1
	Mean ratio of absolute error	0.37	0.39	0.45	0.41	0.50	0.61

TBNK is a total of CD3+ T cells, NK cells and B cells.

Table 6. The evaluation of the static predictive model in distinguishing sepsis and non-sepsis patients.

	Sepsis (n = 14)	Non-sepsis (n = 84)	p value
Site			0.2369
Peumonia, n (%)	9 (64.29%)	49 (58.33%)	
Urinary infection, n (%)	2 (14.29%)	27 (32.14%)	
Other infection, n (%)	3 (21.43%)	8 (9.52%)	
Pathogen			0.0005
Bacteria, n (%)	5 (35.71%)	19 (22.62%)	
Virus, n (%)	3 (21.43%)	8 (9.52%)	
Fungi, n (%)	5 (35.71%)	6 (7.14%)	
Unidentified, n (%)	1 (7.14%)	51 (60.71%)	
PBLS distribution			
TBNK, cells/μL	576.10 ± 376.10	1139.00 ± 498.80	0.0001
CD3+ T cells, cells/μL	457.10 ± 308.30	856.80 ± 405.30	0.0004
CD4+ T cells, cells/μL	211.00 ± 156.50	411.50 ± 239.10	0.0014
CD8+ T cells, cells/μL	212.30 ± 153.50	397.20 ± 197.40	0.0004
NK cells, cells/μL	59.52 ± 31.49	171.80 ± 129.30	0.0003
B cells, cells/μL	46.58 ± 51.47	96.44 ± 61.57	0.0006
Percentile in predicted interval (%)			
TBNK	11.79 ± 9.53	35.60 ± 26.77	0.0014
CD3+ T cells	14.63 ± 13.37	35.95 ± 27.73	0.0060
CD4+ T cells	16.07 ± 18.93	35.12 ± 28.50	0.0179
CD8+ T cells	16.79 ± 18.36	36.90 ± 28.54	0.0125
NK cells	12.14 ± 8.71	43.57 ± 29.61	0.0002
B cells	18.93 ± 27.05	37.80 ± 27.77	0.0202

TBNK is a total of CD3+ T cells, NK cells and B cells. PBLSs, peripheral blood lymphocyte subpopulations.

was significantly lower than in the static model ($p < 0.001$), indicating a more precise prediction for infected RTRs with the dynamic model. However, predictions for B cells were less accurate, with the highest mean ratio of absolute error at 0.61, suggesting that B cells were less influenced by the dynamic indicators during infection.

In summary, the static predictive model could aid in distinguishing infected RTRs from stable RTRs, while the dynamic predictive model remained applicable for predicting PBLSs in infected RTRs.

4. Discussion

In this study, machine learning models were developed using a large dataset to accurately predict reference values for PBLSs in stable RTRs at any time point after transplantation. Both static and dynamic indicators impacting PBLS reconstitution were identified and incorporated into the models. The static predictive model provided insights into PBLS reconstitution under typical conditions and revealed patterns of immune recovery, while also aiding in distinguishing infected RTRs from stable ones. The dynamic predictive model further enhanced predictive performance, particularly in terms of precision. These predictive models were available for free at http://pbls.kqxu.com/.

Tailoring immunosuppressive regimens based on individual immune status is a promising strategy. PBLSs, as key components of the immune system, are primary targets for immune monitoring. Numerous studies have established correlations between PBLSs and post-transplant complications [1,2,17]. Persistent CD4+ T cell lymphopenia, defined as CD4+ T cell counts < 300 cells/μl one year post-transplant, has been associated with higher rates of opportunistic infections, cancers, and mortality [7,18]. Kinetic monitoring of PBLSs post-transplant showed that a CD8+ T cell count < 100 cells/μl at one month in the non-ATG group, and a CD4+ T cell count < 50 cells/μl at one month in the ATG group, had strong negative predictive values for opportunistic infections [8]. Our team also reported a significant reduction in PBLS counts, rather than percentages, in RTRs with pneumonia,

and developed machine learning models to identify pneumonia patients based on CD8$^+$ T cells, NK cells, and overall TBNK cell counts [6].

Despite the importance of PBLS monitoring, no studies have used PBLSs to guide immunosuppressive drug adjustments. In a randomized controlled trial (RCT), immunosuppression modification was based on an immune response assay for liver transplant recipients [19]. The result of the ImmuKnow assay, which detected cell–mediated immunity by measuring the concentration of adenosine triphosphate (ATP) from CD4$^+$ T cells after stimulation, determined the adjustment of tacrolimus dose in the interventional group. The 1–year patient survival was significantly higher and the incidence of bacterial and fungal infections was lower in the interventional group. In addition, the tacrolimus dosage was also lower in the interventional group [19]. Although similar assays have been used to predict infection or rejection in kidney transplantation, no interventional RCTs have been reported [20–22]. The torque teno virus (TTV), an apathogenic virus reflecting immune function, is a promising marker for guiding immunosuppressive adjustments, with a multicenter interventional phase II RCT currently underway [23].

A significant limitation of PBLS monitoring is the lack of standardized reference values post-transplant. Without accurate reference values, modifying immunosuppressive therapy based on PBLSs is challenging. The predictive models developed in this study offer highly personalized PBLS reference values. One critical application of these models is to flag potential over-immunosuppression during follow-up. When PBLS values fall significantly below predicted levels, it may serve as an indicator for adjusting immunosuppressive therapy.

The study also investigated patterns of immune reconstitution, with transplant time and induction therapy identified as the most influential factors. Induction therapy significantly reduced all PBLS subsets at transplant, with most subsets, except B cells, rapidly increasing and reaching a plateau within three months in stable RTRs. ATG had the most profound and prolonged effect on CD4$^+$ T cells, consistent with previous studies [9,24]. PBLS recovery was faster and cell counts were higher in this study compared to previous reports, likely due to lower ATG doses and maintenance levels of CNIs [8,9,12]. B cells, however, exhibited a distinct pattern, peaking sharply around two weeks post-transplant and gradually declining to a plateau at approximately four months. Low-dose ATG has been reported to enhance B cell proliferation while inhibiting differentiation in vitro [25]. The use of basiliximab as induction therapy similarly increased peripheral B cells within one month post-transplant, with recovery at three months, mirroring the trends observed in our results [26]. The consistent reconstitution pattern of B cells across all static model stratifications suggests it may be induced by the transplant itself, warranting further investigation into the mechanisms and changes in B cell subpopulations.

This study has limitations. All patients were recruited from a single transplant center, and validation using external data from other centers is anticipated. Additionally, the majority of patients received grafts from deceased donors and were maintained on tacrolimus, which may limit the model's accuracy for RTRs receiving grafts from living relatives or maintained on CsA. Due to the limited number of cases, alternative immunosuppressive regimens, such as MMF withdrawal, were not included in the model, although these regimens may significantly affect immune reconstitution. In addition, induction therapy dosing, particularly for ATG, may vary across centers. As ATG strongly reduces lymphocyte counts, suboptimal dosing could influence the model's performance in different patient populations.

Disclosure statement

The authors of this manuscript have no conflicts of interest to disclose as described by the American Journal of Transplantation. None of the organs were procured from executed prisoners and that organs were procured after informed consent or authorization.

Funding

ORCID

Yingzi Ming   http://orcid.org/0009-0009-8878-3831

Data availability statement

The datasets used and/or analyzed during the current study are available from the corresponding author on reasonable request.

References

[1] Dendle C, Mulley WR, Holdsworth S. Can immune biomarkers predict infections in solid organ transplant recipients? A review of current evidence. Transplantation Reviews (Orlando, Fla). 2019;33(2):87–98. doi: 10.1016/j.trre.2018.10.001.

[2] Fernández-Ruiz M, López-Medrano F, Aguado JM. Predictive tools to determine risk of infection in kidney transplant recipients. Expert Rev Anti Infect Ther. 2020;18(5):423–441. doi: 10.1080/14787210.2020.1733976.

[3] Jimenez-Coll V, Llorente S, Boix F, et al. Monitoring of serological, cellular and genomic biomarkers in transplantation, computational prediction models and role of cell-free DNA in transplant outcome. Int J Mol Sci. 2023;24(4):3908. doi: 10.3390/ijms24043908.

[4] Boix F, Jimenez-Coll V, Legaz I, et al. Higher expression of activated CD8(+) T lymphocytes (CD8(+)CD25(+), CD8(+)CD69(+) and CD8(+)CD95(+)) mediate early post-transplant acute tubular injury in kidney recipients. Front Biosci (Landmark Ed). 2023;28(6):119. doi: 10.31083/j.fbl2806119.

[5] Alfaro R, Martínez-Banaclocha H, Llorente S, et al. Computational prediction of biomarkers, pathways, and

new target drugs in the pathogenesis of immune-based diseases regarding kidney transplantation rejection. Front Immunol. 2021;12:800968. doi: 10.3389/fimmu.2021.800968.

[6] Peng B, Gong H, Tian H, et al. The study of the association between immune monitoring and pneumonia in kidney transplant recipients through machine learning models. J Transl Med. 2020;18(1):370. doi: 10.1186/s12967-020-02542-2.

[7] Ducloux D, Courivaud C, Bamoulid J, et al. Prolonged CD4 T cell lymphopenia increases morbidity and mortality after renal transplantation. J Am Soc Nephrol. May. 2010;21(5):868–875. doi: 10.1681/ASN.2009090976.

[8] Fernández-Ruiz M, López-Medrano F, Allende LM, et al. Kinetics of peripheral blood lymphocyte subpopulations predicts the occurrence of opportunistic infection after kidney transplantation. Transpl Int. 2014;27(7):674–685. doi: 10.1111/tri.12321.

[9] Longuet H, Sautenet B, Gatault P, et al. Risk factors for impaired CD4+ T-cell reconstitution following rabbit antithymocyte globulin treatment in kidney transplantation. Transpl Int. 2014;27(3):271–279. doi: 10.1111/tri.12249.

[10] Zhang K, Wang F, Zhang M, et al. Reference ranges of lymphocyte subsets balanced for age and gender from a population of healthy adults in Chongqing District of China. Cytometry B Clin Cytom. 2016;90(6):538–542. doi: 10.1002/cyto.b.21323.

[11] Bonnefoy-Bérard N, Vincent C, Revillard JP. Antibodies against functional leukocyte surface molecules in polyclonal antilymphocyte and antithymocyte globulins. Transplantation. 1991;51(3):669–673. doi: 10.1097/00007890-199103000-00024.

[12] Gurkan S, Luan Y, Dhillon N, et al. Immune reconstitution following rabbit antithymocyte globulin. Am J Transplant. 2010;10(9):2132–2141. doi: 10.1111/j.1600-6143.2010.03210.x.

[13] Huang J, Wang H, Fan ST, et al. The national program for deceased organ donation in China. Transplantation. 2013;96(1):5–9. Jul 15. doi: 10.1097/TP.0b013e3182985491.

[14] Peng B, Yang M, Zhuang Q, et al. Standardization of neutrophil CD64 and monocyte HLA-DR measurement and its application in immune monitoring in kidney transplantation. Front Immunol. 2022;13:1063957. doi: 10.3389/fimmu.2022.1063957.

[15] Branch of Organ Transplantation of Chinese Medical A. Branch of Organ Transplantation of Chinese Medical Association Process and specification of Chinese donation after citizen's death (2019 edition). Organ Transplantation. 2019;10(2):122–127. doi: 10.3969/j.issn.1674-7445.2019.02.003.

[16] Huang J, Millis JM, Mao Y, et al. Voluntary organ donation system adapted to Chinese cultural values and social reality. Liver Transpl. 2015;21(4):419–422. doi: 10.1002/lt.24069.

[17] Fernández-Ruiz M, Kumar D, Humar A. Clinical immune-monitoring strategies for predicting infection risk in solid organ transplantation. Clin Transl Immunology. 2014;3(2):e12. Feb. doi: 10.1038/cti.2014.3.

[18] Ducloux D, Carron PL, Racadot E, et al. CD4 lymphocytopenia in long-term renal transplant recipients. Transplant Proc. 1998;30(6):2859–2860. doi: 10.1016/s0041-1345(98)00843-4.

[19] Ravaioli M, Neri F, Lazzarotto T, et al. Immunosuppression Modifications Based on an Immune Response Assay: results of a Randomized, Controlled Trial. Transplantation. 2015;99(8):1625–1632. doi: 10.1097/TP.0000000000000650.

[20] He J, Li Y, Zhang H, et al. Immune function assay (ImmuKnow) as a predictor of allograft rejection and infection in kidney transplantation. Clin Transplant. 2013;27(4):E351–8. doi: 10.1111/ctr.12134.

[21] Mian M, Natori Y, Ferreira V, et al. Evaluation of a novel global immunity assay to predict infection in organ transplant recipients. Clin Infect Dis. 2018;66(9):1392–1397. doi: 10.1093/cid/cix1008.

[22] Naderi H, Pourmand G, Dehghani S, et al. Monitoring cellular immune function of renal transplant recipients based on adenosine triphosphate (ATP) production by mitogen-induced CD4+ T helper cells. Biomed Pharmacother. 2018;107:1402–1409. doi: 10.1016/j.biopha.2018.08.110.

[23] Haupenthal F, Rahn J, Maggi F, et al. A multicentre, patient- and assessor-blinded, non-inferiority, randomised and controlled phase II trial to compare standard and torque teno virus-guided immunosuppression in kidney transplant recipients in the first year after transplantation: TTVguideIT. Trials. 2023;24(1):213. doi: 10.1186/s13063-023-07216-0.

[24] Müller TF, Grebe SO, Neumann MC, et al. Persistent long-term changes in lymphocyte subsets induced by polyclonal antibodies. Transplantation. 1997;64(10):1432–1437. Nov 27. doi: 10.1097/00007890-199711270-00010.

[25] Klaus P, Heine G, Rasche C, et al. Low-dose anti-thymocyte globulin inhibits human B-cell differentiation into antibody-secreting cells. Acta Derm Venereol. 2015;95(6):676–680. doi: 10.2340/00015555-2046.

[26] Longshan L, Dongwei L, Qian F, et al. Dynamic analysis of B-cell subsets in de novo living related kidney transplantation with induction therapy of basiliximab. Transplant Proc. 2014;46(2):363–367. doi: 10.1016/j.transproceed.2013.12.033.